land

MDPI

Article

Empirical Modeling of Soil Loss and Yield Utilizing RUSLE and SYI: A Geospatial Study in South Sikkim, Teesta Basin

Md Nawazuzzoha [1], Md. Mamoon Rashid [1], Prabuddh Kumar Mishra [2,*], Kamal Abdelrahman [3], Mohammed S. Fnais [3] and Hasan Raja Naqvi [1,*]

[1] Department of Geography, Faculty of Science, Jamia Millia Islamia, New Delhi 110025, India; md1910184@st.jmi.ac.in (M.N.)
[2] Department of Geography, Shivaji College, University of Delhi, New Delhi 110027, India
[3] Department of Geology and Geophysics, College of Science, King Saud University, Riyadh 11451, Saudi Arabia
* Correspondence: prabuddh@shivaji.du.ac.in (P.K.M.); hnaqvi1@jmi.ac.in (H.R.N.)

Abstract: Soil erosion and subsequent sedimentation pose significant challenges in the Sikkim Himalayas. In this study, we conducted an assessment of the impact of rainfall-induced soil erosion and sediment loss in South Sikkim, which falls within the Teesta Basin, employing Revised Universal Soil Loss Equation (RUSLE) and Sediment Yield Index (SYI) models. Leveraging mean annual precipitation data, a detailed soil map, geomorphological landforms, Digital Elevation Models (DEMs), and LANDSAT 8 OLI data were used to prepare the factorial maps of South Sikkim. The results of the RUSLE and SYI models revealed annual soil loss >200 t ha^{-1} yr^{-1}, whereas mean values were estimated to be 93.42 t ha^{-1} yr^{-1} and 70.3 t ha^{-1} yr^{-1}, respectively. Interestingly, both models displayed similar degrees of soil loss in corresponding regions under the various severity classes. Notably, low-severity erosion <50 t ha^{-1} yr^{-1} was predominantly observed in the valley sides in low-elevation zones, while areas with severe erosion rates >200 t ha^{-1} yr^{-1}were concentrated in the upper reaches, characterized by steep slopes. These findings underscore the strong correlation between erosion rates and topography, which makes the region highly vulnerable to erosion. The prioritization of such regions and potential conservation methods need to be adopted to protect such precious natural resources in mountainous regions.

Keywords: soil erosion; sediment; RUSLE; Himalaya; conservation

check for updates

Citation: Nawazuzzoha, M.; Rashid, M.M.; Mishra, P.K.; Abdelrahman, K.; Fnais, M.S.; Naqvi, H.R. Empirical Modeling of Soil Loss and Yield Utilizing RUSLE and SYI: A Geospatial Study in South Sikkim, Teesta Basin. *Land* **2024**, *13*, 1621. https://doi.org/10.3390/land13101621

Academic Editor: Nick B. Comerford

Received: 16 September 2024
Accepted: 2 October 2024
Published: 5 October 2024

Copyright: © 2024 by the authors. Licensee MDPI, Basel, Switzerland. This article is an open access article distributed under the terms and conditions of the Creative Commons Attribution (CC BY) license (https://creativecommons.org/licenses/by/4.0/).

1. Introduction

Soil is the top layer of the Earth's surface capable of supporting life. Erosion is the geological process through which earthen elements are eroded down and transferred by natural forces such as wind or water. Soil erosion is a global environmental issue that poses major threats to natural resources [1], agriculture [2], and the ecological environment [3,4]. It has a negative economic and environmental impact [5]. Soil erosion reduces soil quality in the detachment area while also producing significant sediment-related issues in the sedimentation area (off-site effect) [6]. Erosion is a phenomenon that takes place in all circumstances and impacts 56% of deteriorated soils worldwide [7]. Inevitably, the increasing worldwide demand for cow products will place strain on fertile soils and exacerbate erosion problems. Hence, the importance of sustainable soil management has become crucial [8]. It is crucial to comprehend soil erosion in order to stop soil degradation, repair damaged soils, and lessen the chance that eroded material would infiltrate ecosystems. Annually, the FAO-led Global Soil Partnership reports that over 75 billion tonnes (Pg) of soil erode from cultivable lands worldwide, resulting in an estimated economic loss of USD 400 billion [9]. Asia produces around 80% of all sediments delivered to the world's oceans, with Himalayan Rivers being the most major producers [10]. Asia also has the highest rate of soil erosion, at 74 tons per acre per year [11]. Approximately 175 million hectares of

land in India, which accounts for about 53% of its geographical area, is susceptible to soil erosion [12]. This degradation accounts for a 1.40% decrease in India's GDP [13]. India experiences an annual average rate of soil erosion of 16.4 tons per hectare, with severe erosion affecting 32.3% of its total geographical area [14].

According to Raymo and Ruddiman, despite covering only about 5% of the Earth's land surface, the Himalayan and Tibetan regions supply approximately 25% of the world's dissolved load [15]. Another study suggested that about 5334 Mt (16.4 ton/hectare) of soil is detached annually in India, with approximately 29% being transported away by rivers into the sea and 10% being deposited in reservoirs, causing a significant loss in storage capacity [16]. Soil erosion rates may fluctuate in response to climate change [17,18] owing mostly to changes in rainfall erosivity [19]. The Himalayan region accounts for over 45% of the total revenue for the local population and serves as a direct or indirect means of subsistence for over 70% of the people living there [20]. Hence, it serves as a significant hindrance in attaining the Sustainable Development Goals (SDGs), namely, Climate Action (SDG 13) and Life on land (SDG 15). Soil erosion has significant consequences, such as reducing biodiversity [21] and microbial diversity and functionality [22]. It also alters nutrient and carbon cycling, leading to a decrease in land productivity, which negatively impacts social well-being [23]. The topsoil, which is crucial for nutrient availability and plant growth, becomes more susceptible to damage from soil erosion [24], leading to reduced soil fertility and productivity [23]. The research region is located in the Himalayan mountain range, which is characterized by geological weakness and fragility, resulting in significant soil erosion conditions [25]. The primary factors contributing to the degradation of land resources in the Himalayan region include soil loss from steep slopes, mudslides, landslides, and the shrinkage of grazing and forest areas [26]. Deforestation, land degradation, and high rainfall have left fragile terrains with steep slopes susceptible to catastrophic soil erosion [23,27]. The varied agricultural systems in Asia, Africa, and South America have documented significant average rates of soil erosion, ranging from 30 to 40 tons per hectare per year. In contrast, India is experiencing an estimated yearly loss of 6.6 billion tons of soil [1]. Multiple field-based investigations conducted in different hydrological units in the Indian Himalayas have described remarkably high erosion rates, ranging from 20–25 t $ha^{-1}yr^{-1}$ to as high as 92 t $ha^{-1}yr^{-1}$ [28–30]. The most susceptible/critical areas for soil erosion are the dry, semi-arid, and sub-humid regions; they also include agricultural areas, mountainous terrain, and the Himalayas [31]. In order to address the challenges of obtaining soil erosion rate measurements over extensive geographical regions, several soil erosion models, such as empirical, semi-empirical, and physical/process-based models, have been utilized [32,33]. The Empirical Universal Soil Loss Equation (USLE) [34], Revised Universal Soil Loss Equation (RUSLE) [35], and Modified Universal Soil Loss Equation (MUSLE) [36] are among the several models available. Semi-empirical models include the Watershed Erosion Prediction Project (WEPP) [37], the Sediment Yield Index (SYI) [38], the Soil and Water Assessment Tool (SWAT) [39], and others. These models differ in terms of the processes taken into account, intricacy, and data prerequisites, and are frequently employed by academics to forecast soil erosion rates at various levels of scale [33]. Despite the superior performance of physically based models, their substantial input requirements (including high spatial resolutions), complexity, and high processing costs have prompted academics and decision makers to increasingly choose empirical models. Extensive studies on soil erosion have been conducted in the Indian Himalayas [17], as well as at many other sites worldwide. To evaluate soil loss, many studies have used the Sediment Yield Index (SYI) or RUSLE models separately [40] or in combination [41]. The assessment of sediment output is becoming important due to the widespread network of dams and reservoirs [42] and is essential for implementing erosion control measures to maintain soil fertility and productivity [43]. For assessing erosion risk at various scales including field [44,45], watershed [46,47], and catchment or regional scales, the RUSLE model has gained exceptional popularity and worldwide acceptance [48–50]. This is particularly true in regions where the applicability of many other complicated models is constrained by the

high costs and input data requirements. The acceptance of RUSLE could be ascribed to its compatibility with remote sensing and GIS as well as its low data requirements and robust model structure [51,52]. SYI stands for sediment yield per unit area, and it is a measure of erosion severity in a watershed. It finds widespread application in research on watershed erosion [53,54]. The SYI is a specialized technique or model employed for the assessment of sediment yield. It entails the allocation of numerical values to individual geomorphological factors, which are subsequently integrated into a mathematical formula to forecast sediment production [4,55]. This SYI model is widely accepted among researchers because of its simplicity and efficiency, requiring fewer data and less time for implementation compared to other models. The accelerated erosion of the young Indian Himalayan range is attributed to its steep and rough topography, shallow soil depth, predominantly coarsely structured soils with limited water storage capacity, continuous agricultural activity along the slopes, and ongoing tectonic movements [56]. There is a conspicuous absence of research on soil erosion in the Himalayas, despite its well-recognized status as a major region for this phenomenon [57,58]. Significantly, the economy of Sikkim is dependent on agriculture. Therefore, soil erosion can lead to the exhaustion of rich topsoil, so reducing agricultural productivity and endangering the means of subsistence for farmers. Despite the benefits of organic farming, soil degradation remains a significant issue in South Sikkim. The confluence of steep slopes and significant precipitation gives rise to soil erosion, consequently culminating in the exhaustion of topsoil abundant in nutrients. There are very few studies on soil erosion in the Sikkim Himalayan region, particularly those that use two empirical models. There are no studies available that explicitly assess the extent of soil erosion in this location. The primary objective of this study is to assess the yearly soil erosion and spatial variation of the degree of severity in South Sikkim using the RUSLE and SYI empirical models. It is imperative to investigate erosion in order to safeguard the environment, improve the local economy, and ensure the well-being of local producers.

2. Materials and Methods

2.1. Study Area

The district of South Sikkim has an area of 754 km^2 extended within the geographical coordinates of 27°14′20″ N latitude and 88°18′15″ E longitude. The South Sikkim district is an important commercial and transport center of the state (Figure 1). It shares its borders with the northern, western, and eastern districts of Sikkim and also shares a southern border with the state of West Bengal. The topography of the district is characterized by high elevations (between 300 and 5000 m), rough terrain, steep slopes, valley side slopes, valleys, and terraces, all of which have different soil types and thicknesses. The soil on the barren, steep slope is shallow and crumbly, whereas the soil in the heavily vegetated sections is rather thick and rich in organic matter. The terraces have granular soils and are quite damp. The northernmost area of the district consists of steep, snow-capped mountains with no human settlements. The majority of the population lives in the center and south of the district at altitudes between 500 and 2500 m. Endless terraces of agricultural land and tiered slopes are interspersed with vernal forests, waterfalls, and breathtaking mountains. The South Sikkim region is characterized by its hilly landscape and a climate that ranges from subtropical to temperate. It receives substantial rainfall, especially during the monsoon season, resulting in abundant flora and a wide range of habitats. South Sikkim has an annual average rainfall of 1625 mm, with temperatures ranging from 17 to 27 °C and lowest temperatures ranging from 2 to 21 °C. The region's climate facilitates many crop patterns, with agriculture serving as the predominant occupation. Farmers mostly participate in the production of crops such as maize, paddy, millet, and various vegetables, as well as engage in horticultural activities such as growing oranges and cardamom, which are essential for the local economy. The region is renowned for its tea plantations, especially in locations such as Temi. The primary population centers in South Sikkim consist of Namchi, the administrative capital of the district, and towns such as Ravangla and Jorethang, which play crucial roles as commercial and administrative hubs. The primary land use patterns in

South Sikkim consist of agricultural lands, forest land, and growing urban developments. Forests are particularly important in preserving the ecological equilibrium and sustaining the renowned biodiversity of the region.

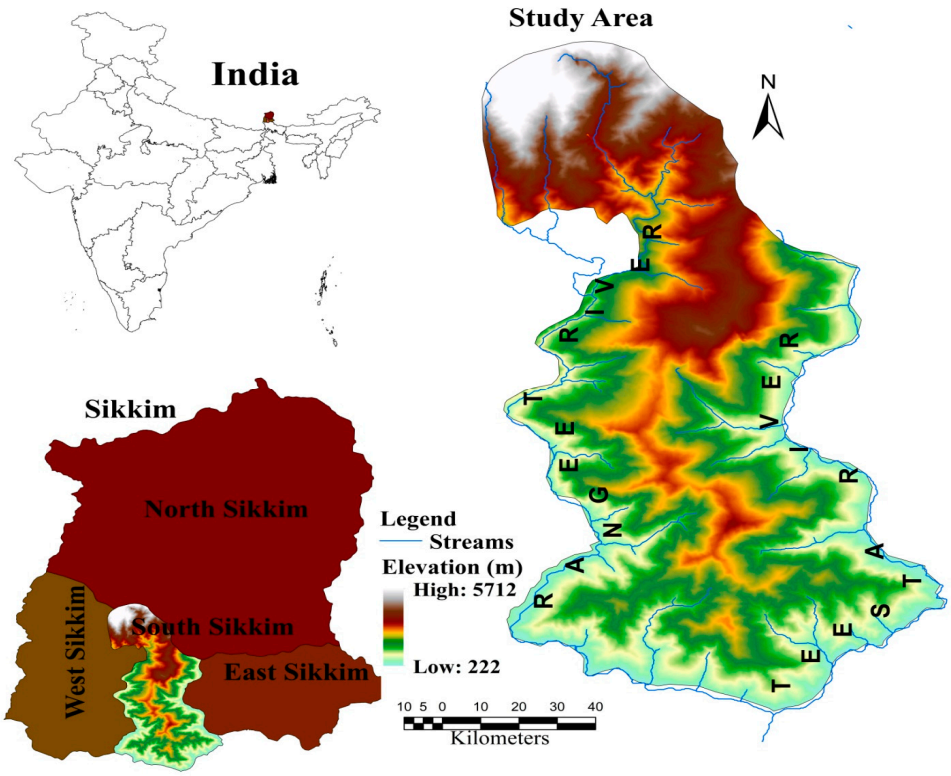


Figure 1. South Sikkim: a part of the Teesta Basin.

2.2. Data and Methods

In order to conduct the research, diverse data sources were employed to generate factorial maps, which served as inputs for the RUSLE and SYI models (Tables 1 and 2). Since the development of new techniques for computing soil erosion variables, the RUSLE has been widely used for both agricultural and forest watersheds to forecast average yearly soil loss [34,35]. It is compatible with a Geographic Information System (GIS), has basic data requirements, and is easy to use and understand [34]. This method has been utilized by researchers worldwide to study soil erosion at various scales [59,60]. The Revised Universal Soil Loss Equation is formalized as Equation (1) [35].

$$A = [R] * [K] * [LS] * [C] * [P] \quad (1)$$

where A represents the annual average of soil loss (t ha^{-1} yr^{-1}), R is the rainfall erosivity factor (MJ mm ha^{-1} h^{-1} yr^{-1}), K is the soil erodibility factor (t h MJ^{-1} mm^{-1}), LS is the slope length and steepness factor (dimensionless), C is the land management factor (dimensionless, ranging from 0 to 1), and P is the conservation support practice factor (dimensionless, ranging from 0 to 1).

Rainfall Erosivity factor (R) was proposed by Wischmeier and Smith as a means to quantify the impact of climate on soil erosion [34]. The precipitation plays a substantial role in soil erosion by means of splash erosion and the movement of runoff. The EI_{30}, which is derived from the comprehensive and long-term records of storm kinetic energy (E) and maximal thirty-minute intensity, is used to calculate the yearly R-factor [35]. Precision assessment of the R-factor requires a minimum of 22 years of rainfall records due to the evident cyclical patterns in rainfall data [34,35]. However, it is generally accepted that 15 years' worth of rainfall data is adequate for accurate estimation [61,62]. On the other

hand, based on data accessibility and local circumstances, a minimum of ten years' worth of rainfall statistics provides a more flexible guideline [63]. In this research, we have used 32 years of average data for rainfall erosivity calculation. The erosivity index in the RUSLE model is generated from the average total erosion of rainfall events per year using Table 1 and Equation (2) [64].

Table 1. Data and methods used for RUSLE model.

Data	Source	Links
Rainfall	IMD	https://www.imdpune.gov.in/cmpg/Griddata/Rainfall_25_NetCDF.html (accessed on 23 May 2024)
Soil Data	FAO	https://www.fao.org/soils-portal/data-hub/soil-maps-and-databases/en/ (accessed on 19 April 2024)
SRTM DEM	NASA	https://www.earthdata.nasa.gov/sensors/srtm (accessed on 15 September 2024)
LANDSAT 8 OLI	USGS	https://earthexplorer.usgs.gov/ (accessed on 12 April 2024)
SRTM DEM	NASA	https://www.earthdata.nasa.gov/sensors/srtm (accessed on 12 April 2024)

Table 2. Conservation practice as per Wischmeier and Smith's data.

Land Use	Slope (%)	P-Factor Value
Agricultural Land	0–5	0.1
	5–10	0.12
	10–20	0.14
	20–30	0.19
	30–50	0.25
	50–100	0.33
Other Land	All	1.00

$$R = \sum_{i=0}^{12} 1.735 \times 10^{(1.5log_{10}(P_i^2/P)-0.08188} \quad (2)$$

where R is rainfall erosivity (MJ mm ha^{-1} h^{-1} $year^{-1}$), P_i is monthly rainfall (mm), and P is annual rainfall (mm). Interpolation of rainfall erosivity values was performed in ArcGIS 10.8 using the Inverse Distance Weighted (IDW) approach, which is a deterministic spatial interpolation technique that utilizes neighboring known values (sample points) to construct estimates for unknown values at certain places. The fundamental concept underlying IDW is that points in closer proximity to the forecast location exert a more pronounced impact on the projected value compared to points located at a greater distance. The approach operates under the premise that the influence of the variable being interpolated diminishes as the distance from the known sites increases.

Soil Erodibility (K) factor maps were constructed using FAO soil maps that were clipped with the study region, and pixels within the study area were identified using soil codes. The K-factor is regulated by the soil layer's organic content, soil texture, structure, and permeability [65]. This research utilized the Harmonized Global Soil Database (HWSD) version 1.2, as specified in FAO/IIASA/ISRIC/ISS-CAS/JRC 2009 (Table 1). The HWSD and its geographical layer can be directly imported as well as read into popular GIS tools for modeling purposes. The determination of this component is derived from data in Table 1 and the Equation (3) proposed by Sharpley and Williams [66].

$$K = (fcsand * fsi - cl * forgc * fhisand * 0.1317) \quad (3)$$

where

$$\text{fcsand} = \left[0.2 + 0.3\exp\left(-0.0256\text{SAN}\left(\frac{1-\text{SIL}}{100}\right)\right)\right] \quad (4)$$

$$\text{fsi} - \text{cl} = \left(\frac{\text{SIL}}{(\text{CLA}+\text{SIL})}\right)^{0.3} \quad (5)$$

$$\text{forgc} = \left[1.0 - \left(\frac{0.25\text{C}}{\text{C}+\exp(3.72-2.95\text{C})}\right)\right] \quad (6)$$

$$\text{fhisand} = \left[1.0 - \left(\frac{0.70\text{SN1}}{\text{SN1}+\exp(-5.51+22.9\text{SN1})}\right)\right] \quad (7)$$

where SAN, SIL, and CLA are percentages of sand, silt, and clay, respectively; C is the organic carbon content; and SN1 is the sand content subtracted from 1 and divided by 100. Fcsand is a soil erodibility factor with a low value. Fsi–cl denotes a low soil erodibility factor with high clay to silt ratio. Forgc is a soil erodibility reducing factor for soil with a high organic content. Fhisand is a component that lowers soil erodibility in sandy soils.

Slope Length and Steepness (LS) factor analyzes the specific influences of topography on soil erosion as the product of slope length (L) and steepness (S), both of which are estimated using DEM. As slope length (L) grows, overall soil erosion and soil erosion per unit area generally intensify due to the progressive buildup of runoff in the down slope direction. As the slope steepness (S) increases, the velocity and erosivity of runoff also accelerate [35,67,68]. Our study employed a Digital Elevation Model (DEM) acquired from the Shuttle Radar Topography Mission (SRTM) with a resolution of 30 m (Table 1). The LS-factor was calculated using Equation (8), proposed by Moore and Burch [69,70].

$$\text{LS} = \left(\text{Flow accumulation} * \frac{\text{cell size}}{122.13}\right)^{0.4}\left(\sin * \frac{\text{slope}}{0.0896}\right)^{1.3} \quad (8)$$

where LS is the total slope length and steepness factor, and flow accumulation determines the area that contributes to an upslope in a specific cell; for this study, the resolution of the DEM is 30 m. Sin slope is the slope degree value in sin [69,70].

Cover Management (C) factor evaluates all vegetative cover and management variables. It can range from 0.001 for dense woods to 1.0 for bare land and is the ratio of soil loss from specific farming to clean-tilled, continuous fallow areas. This study also assessed the C-factor using satellite remote sensing data [71]. This calculation used the Normalized Difference Vegetation Index (NDVI), which measures vegetation health and vigor. We used the Colman Equation (9) for C and it is calculated from LANDSAT8OLI data (Table 1) [72].

$$\text{C}_{\text{rA}} = 0.1 * \frac{-\text{NDVI}+1}{2} \quad (9)$$

where C_{rA} is the estimated C-factor.

The **Conservation Practice (P)** factor compares soil loss from one conservation practice to up and down slope farming [34]. It shows how contour farming, strip cropping, and terracing affect soil loss at a specific site by changing the flow pattern or direction of surface runoff by reducing volume and runoff rate [73]. Many sites use contour cropping and terracing to control erosion, whose values range from 0 to 1 [74]. Soil erosion management is better with a lower P-factor. Contour cultivation, strip cropping, and terracing increase the P-factor compared to natural erosion [40]. The LULC map from LANDSAT 8OLI data (Table 1) is used in this research to fulfill the conservation practice criteria (Table 2).

The SYI model offers criteria for prioritizing the delineation of river valleys based on the Sediment Yield Indexmodel created by the All India Soil and Land Use Survey [55] using Equation (10).

$$\text{Seiment Yield Index} = \frac{\sum(\text{A}_\text{i} \times \text{W}_\text{i} \times \text{D}_\text{i})}{\text{A}_\text{w}} \times 100 \quad (10)$$

where A_i is the area of the ith mapping unit; W_i is the weightage assigned to the ith unit; D_i is the delivery ratio assigned to the ith unit, which is calculated using Equation (11) by Williams and Berndt [75]; A_w is the total area of the watershed/sub-watershed. The below Equation (11) is used to calculated the delivery ratio (D_i) parameter of the SYI model.

$$SDR = 0.627 * (slope)^{0.403} \quad (11)$$

To conduct this study, we acquired rainfall data from the India Meteorological Department (IMD) to determine the Rainfall Erosivity (R) factor. Soil data were acquired from the Food and Agricultural Organization (FAO) to compute soil erodibility values (K-factor) using the methodologies outlined by [76]. We utilized the Shuttle Radar Topography Mission (SRTM) Digital Elevation Model (DEM) 30m data provided by the USGS to extract elevation, delivery ratio (DR) equation (11), and slope length and steepness. Furthermore, the LANDSAT 8 OLI imagery of the year 2022 was utilized to create Land Use Land Cover (LULC) data and generate the Normalized Difference Vegetation Index (NDVI). These data were subsequently applied to determine the Crop Cover (C) and Practice Management (P) factors within the context of the RUSLE model. The workflow, which utilizes different data and equations to quantify sediment loss through both models, is demonstrated in Figure 2 and Table 1, respectively.

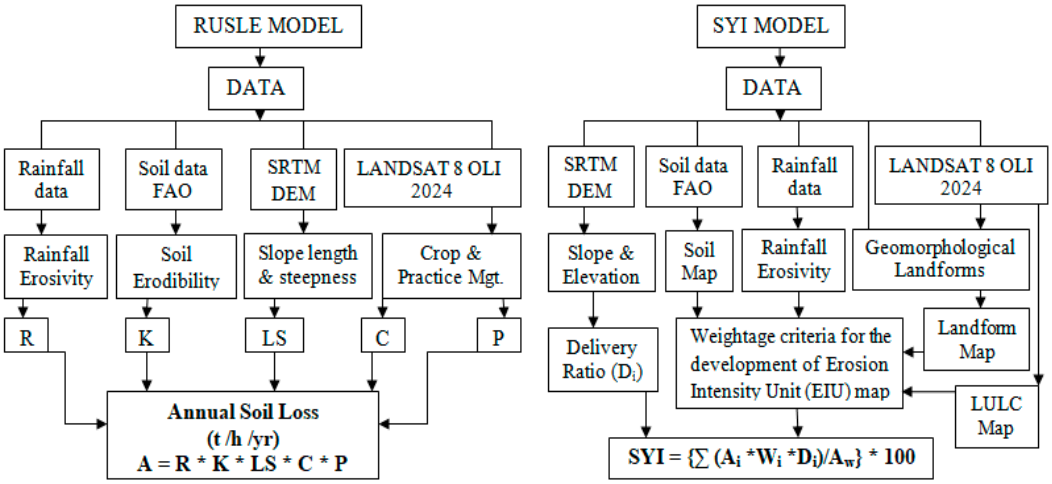


Figure 2. Schematic flow chart of the methodology adopted for sediment loss quantification employing RUSLE and SYI empirical models.

The erosion and deposition process depends on the nature and characteristics of the surface. Hence, the slope and vegetation covering the surface of a region play a pivotal role in governing soil erosion [60,77,78]. In accordance with AISLUS recommendations, erosion intensity units for the SYI model were calculated based on factors including slope, elevation, land use land cover, soil type, rainfall erosivity, and the delivery ratio determined by drainage length (Table 3). The weightage scores (10 to 50) for each class under different factors was determined as per the erosion potential/vulnerability. Later, the mean sediment loss values of both the RUSLE and SYI models were averaged to determine the severity zones and ranks of the study area.

Table 3. SYI model: method and data with their sources.

Equations	Factors	Data	Source
A_i	Area of ith Unit		
W_i	Slope	SRTM DEM 30m	NASA
	Rainfall Erosivity	Rainfall	IMD
	LULC	LANDSAT 8 OLI	USGS
	Elevation	SRTM DEM 30m	NASA
	Soil	Digital Soil Map of the World (2019)	FAO
	Landforms	Geomorphical Landforms	GSI
D_i	Delivery Ratio	SRTM DEM30m	NASA
A_w	Total Area of a Region		

3. Results and Discussion

3.1. Mapping of Parameters in RUSLE Model

Various criteria and equations were employed in the creation of factorial layers, which involved the computation of annual soil loss through the RUSLE model. The equation and references for each factor of the RUSLE are mentioned in Table 1. To calculate the R-factor, 32 years of mean annual rainfall data of the study area from the Indian Meteorological Department were used as per the equation mentioned in Table 1. The Inverse Distance Weightage (IDW) interpolation method was used to create a 30 × 30 pixel size that computed rainfall erosivity ranging from 2043 to 4669 MJ mm ha^{-1} h^{-1} yr^{-1}, which is comparatively high and somewhat close to the rainfall erosivity values in the nearby Papung Khola Sub-watershed [60]. The rainfall erosivity is high in the southeastern part, moderate in the central part, and comparatively lower in the northwestern region of the study area (Figure 3a). The term "soil erodibility factor" (K) describes a soil's inherent propensity to be eroded by rainfall and runoff. The permeability of the soil layer, soil structure, organic content, and soil texture all influence the K-factor [65]. The FAO soil map was used to construct the soil erodibility factor map, which was then clipped with the study area, and the pixels within the study region were identified using the soil code. Soil erodibility values were determined for various soil types, taking into consideration factors such as soil texture, permeability, and the antecedent moisture content of the soil. The "k" factor, represented by a numerical scale ranging from 0 to 1, indicates the degree of soil erodibility, with lower values indicating a reduced susceptibility to soil erosion. This factor is calculated using the equation presented by Kouli in Table 1. [76]. The different soil types found in the area are lithosol, dystric cambisols, dystric regosol, humic acrisol, and gleysol. There are two distinctive erodibility values i.e., 0.105 and 0.154 Mg $ha^{-1}MJ^{-1}mm^{-1}$, where a higher value indicates more susceptibility to erosion (Figure 3b). The dominant soil type is lithosol and dystric cambisols, which has a K value of 0.154 and covers approximately 80% of the area. The interplay between soil erosion and terrain gradient is modulated by factors such as vegetation cover and soil particle size. As the Slope Steepness (S) rises, both the velocity and erosive potential of runoff escalate, as documented in studies by Renard and Lastoria [35,68]. We employed 30m resolution DEM data for LS-factor mapping using the formula introduced by Moore and Burch mentioned in Table 1 [69,70]. The dimensionless LS-factor assesses the combined influence of Slope Length (L) and Steepness (S), which are derived from Digital Elevation Models (DEMs), in order to quantitatively measure the impact of topography on soil erosion. The colors other than yellow patches show values greater than 20 in the LS-factor map, depicting the great potential of soil erosion. The region has mountainous and hilly topography that has a relatively large slope with a length (>60) compared to the plain region. The northern and southeastern sections of this area exhibit relatively high LS values when compared to the eastern and southern portions. Low LS values (<20) are scattered in patches across the region, with a predominant concentration in the central area (Figure 3c). The Crop or Land Cover Management Factor (C) quantifies the impact of vegetation and ground cover on soil erosion potential. It is defined as the

ratio of soil loss from specific farmland in comparison to the soil loss from clean-tilled, continuous fallow areas. Typically, this value ranges from 0.001 for dense woods to 1.0 for bare land [34,79]. The C-factor was generated using the NDVI extracted from LANDSAT 8 OLI data from the year 2022, employing the equation provided by Colman [80]. In this study, the computed C values span from 0.042 to 0.078, closely approaching zero, which suggests a predominance of substantial land cover or robust vegetation. Notably lower C values are observed in the predominantly snowy northern region, with a few patches exhibiting similar trends in the central and southern areas (Figure 3d).

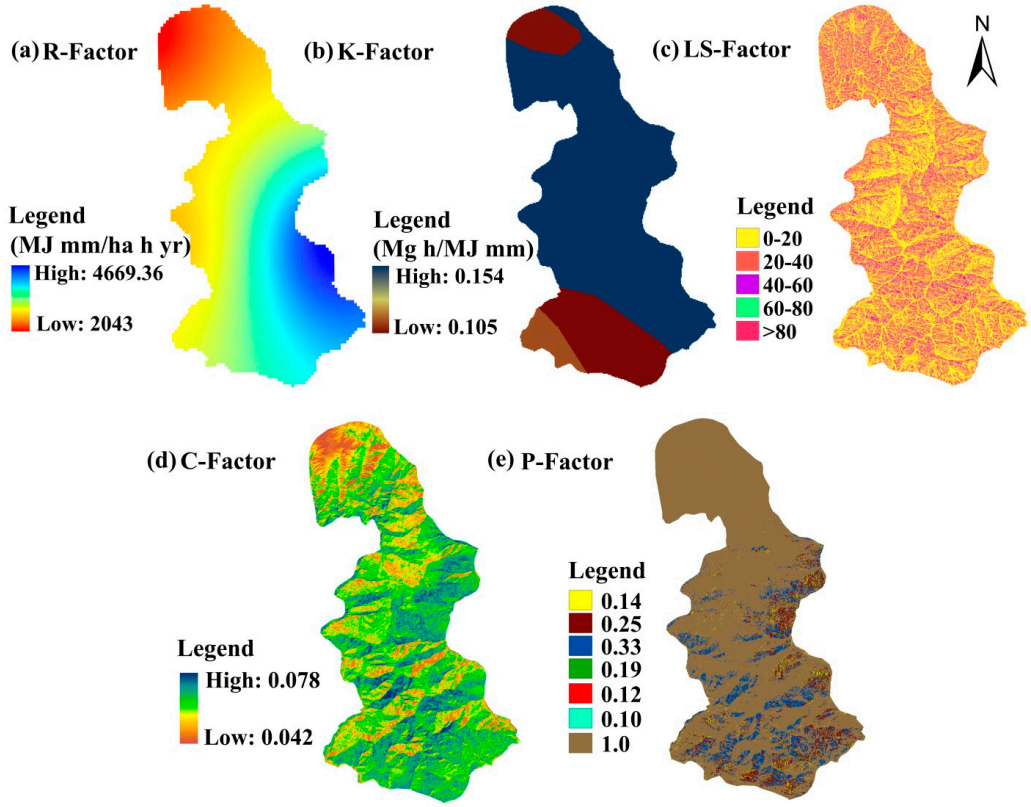


Figure 3. Factors mapping: Rainfall Erosivity (**a**), Soil Erodibility (**b**), Slope Length and Steepness (**c**), Cover Management, (**d**) and Support Practice (**e**) factors of RUSLE model.

The Conservation Practice Factor (P) signifies the ratio of soil loss after implementing a specific support practice to the initial soil loss, serving as a metric to quantify the impact of soil and water conservation measures. The P-factor ranges from 0 to 1, with a lower value indicating the effectiveness of conservation practices. Because of the limited availability of dependable data regarding the conservation practices employed by farmers and the potential absence of enduring management techniques, we have created the Land Use and Land Cover (LULC) map and the slope map. These maps have been integrated with the criteria established by Wischmeier and Smith for calculating the P-factor, as outlined in Table 2 [34]. Based on the Land Use and Land Cover (LULC) map, the dominant agricultural practices are observed in the southern, southeastern, and southwestern parts of this region. In these areas, the majority of agricultural land falls within the 50–100% slope category, exhibiting a p value of 0.33. This indicates a relatively low level of conservation practices compared to the other parts of the region. Conversely, the regions characterized by a (0–5) % slope, with a p value of 0.1, demonstrate notably higher levels of practice management (Figure 3e).

3.2. Mapping of Parameters for SYI Model

Very few studies have employed the SYI model to calculate the sediment yield, recommended by the All India Soil and Land Use Survey [55]. These studies involved the determination of an Erosion Intensity Mapping Unit (EIMU) for the region. This mapping unit was established through the integration of various data sources, including factors that influence erosion intensity, such as slope, rainfall, elevation, Land Use and Land Cover (LULC), lithology, and geomorphological landforms. We evaluated various key parameters across distinct categories and allocated weightage scores in accordance with previous research findings [81,82]. The weightage value was allocated to each theme based on the significance of its features within the region.

In the study area, the slope was categorized into five classes (Figure 4a), and higher weightage values were assigned to the higher slopes as they have significantly high potential for erosion (Table 4). The maximum area lies in the category of a greater than 20 degree slope, while the <10 degree slope category occupies a comparatively smaller region. The high weightage scores were determined for those regions where the slope (in degree) is also high that have great erosion potential (Table 4 and Figure 4b). The weightage value increases as the rainfall erosivity becomes more pronounced according to the five classes, ranging from 2000 MJ mm/ha h yr to over 4000 MJ mm/ha h yr. In this classification, the least weightage value was assigned to low erosivity, while the highest scores were assigned to high rainfall erosivity (Table 4 and Figure 4b). Moreover, the elevation factor was also integrated into the analysis of the region that was divided into five distinct zones, spanning from 222 m to over 4000 m, and accordingly, the weightage values were assigned in ascending order to the highest class (Table 4 and Figure 4c). The sediment is directly influenced by various Land Use and Land Cover (LULC) categories due to their interactions with soil and water. In this context, we identified five distinct LULC classes. Among these classes, vegetation stands out as the predominant one, receiving a score of 30. Snow cover, water bodies, and settlements were assigned a score of 10 each. On the other hand, bare land and agricultural land received a higher score as these covers have great potential for runoff in mountainous regions (Table 4 and Figure 4d). Similarly, the different soils were identified as lethosol, gleysol, dystric cambisols, and dystric regosols along with their weightage scores, which are lower than humic acrisol soil (Table 4 and Figure 4e). In terms of geomorphology, the predominant features in the study region consist of moderately dissected hills and valleys, as well as highly dissected hills and valleys, making it more susceptible to erosion (Table 4 and Figure 4f). Some weightage values were derived from previously published literature, as exemplified in works by Lohar and Kumar [52,83]. The delivery ratio has been computed using the nearest stream's (drainage density) distance, measured in kilometers. Delivery ratio values were allocated based on the stream's length. In the study area, the majority of micro watersheds were assigned delivery ratio values of 0 and 1 in accordance with the drainage density [4].

Table 4. Integrated factors along with their weightage scores for SYI model.

Factors	Class for (W_i)	Assigned Weightage Value
Slope	0–10	10
	10–20	20
	20–30	30
	30–40	40
	>40	50
Rainfall Erosivity	2000–2500	10
	2500–3000	20
	3000–3500	30
	3500–4000	40
	>4000	50

Table 4. *Cont.*

Factors	Class for (W_i)	Assigned Weightage Value
LULC	Snow Cover	10
	Bare Land	50
	Vegetation	30
	Water Bodies	10
	Settlement	10
	Agriculture Land	40
Elevation	222–600	10
	600–1800	20
	1800–3000	30
	3000–4000	40
	>4000	50
Soil	Lithosol	30
	Gleysol	10
	Dystric Cambisols	20
	Humic Acrisols	50
	Dystric Regosols	40
Geomorphological Landform	Terrace	20
	Valley	10
	Active Flood Plain	10
	Moderately Dissected Hills and Valley	30
	Highly Dissected Hills and Valley	40
	Snow Cover	10
	River	10
	Landslide	40

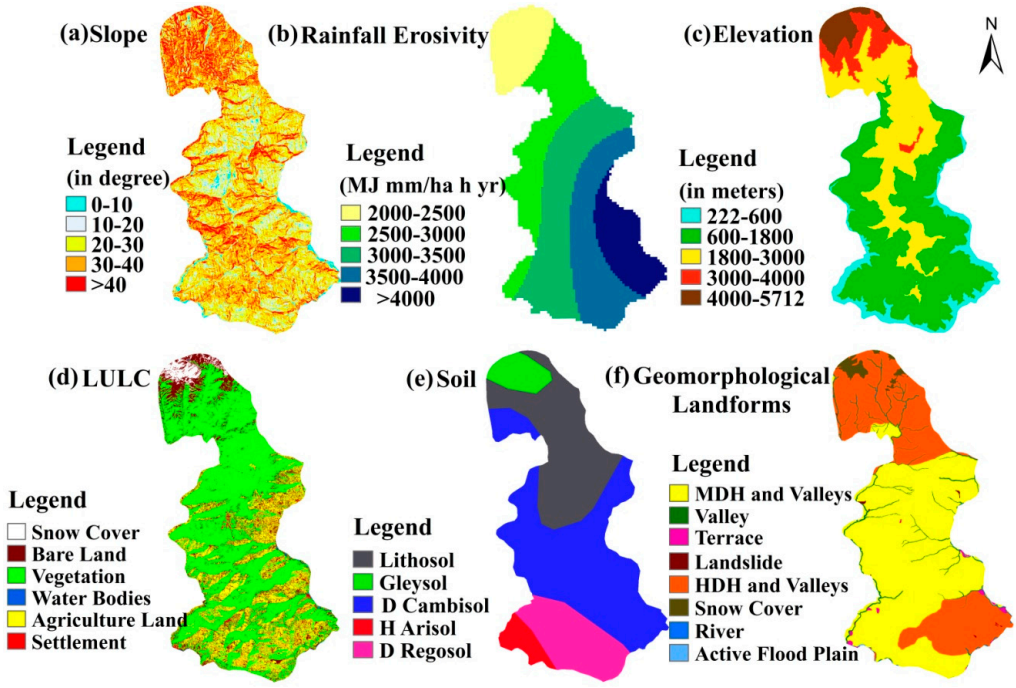


Figure 4. Factors employed for SYI model: slope in degree (**a**), rainfall erosivity (**b**), elevation (**c**), LULC (**d**), soil (**e**), and geomorphological landforms in which there are MDHs, Moderately Dissected Hills, and HDHs, Highly Dissected Hills (**f**).

3.3. Quantifying Erosion Using RUSLE and SYI Models

In both the RUSLE and SYI models, the soil loss rate was classified into five classes, which ranged from <50 t $ha^{-1}yr^{-1}$ to >200 t ha^{-1} yr^{-1}. In the context of the RUSLE model, our approach for determining the mean soil loss across the entire area involved the calculation of a weighted average using the calculated annual soil loss values and their corresponding area percentages. As per the RUSLE model, the mean amount of soil loss in the area is approximately 93.42 t $ha^{-1}yr^{-1}$. Most of the area (46.42%) has a low soil loss rate <50 t $ha^{-1}yr^{-1}$ that is characterized by a low elevation zone. The area has a severe erosion rate >200 t $ha^{-1}yr^{-1}$ concentrated at the upper reaches of the northern part that covers 20% area, where the Slope Length (L) and steepness are high (Table 5 and Figure 5a). A few pixels under the high rate of erosion were also identified in the central parts of the area. A high to very high rate of soil erosion, > 150 t $ha^{-1}yr^{-1}$, was observed in the west-central and southern regions, which together make up 19% of the area. Sporadic instances of this category were also identified in the northern part.

Table 5. RUSLE and SYI model-based comparative statistical analysis and level of severity under erosion rate classes.

Rate of Erosion and Sediment Yield t/h/y	RUSLE Area (km^2)	RUSLE Area %	SYI Area (km^2)	SYI Area%	Severity Level
<50	339.54	46.42	258.2	35.30	Very Low
50–100	109.13	14.92	120.69	16.5	Low
100–150	73.0	9.98	172.64	23.6	Moderate
150–200	64.6	8.83	66.13	9.04	High
>200	145.2	19.85	113.81	15.56	Very High

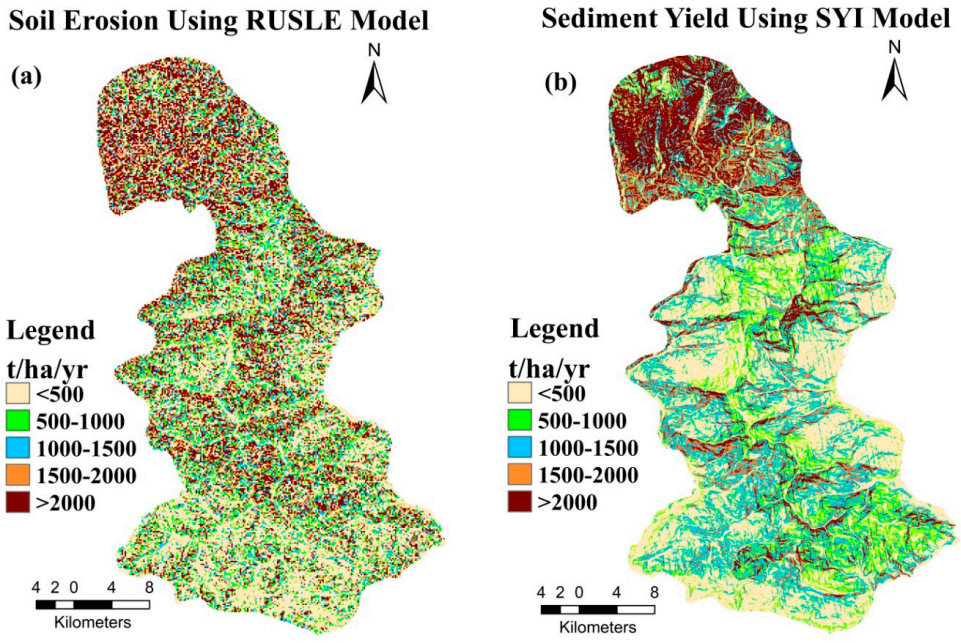


Figure 5. RUSLE (**a**) and SYI (**b**) empirical model-based soil loss rate.

The SYI model estimates that the average sediment yield across the entire area is approximately 70.30 t $ha^{-1}yr^{-1}$. The categorized statistics showed that about 35% of the land is situated within the low soil loss risk category (<50 t $ha^{-1}yr^{-1}$), primarily found in areas with low elevation and the lowest effects of slope steepness. Moderate sediment yield risk covers 16.5% of the land area with sediment yields ranging between 50 and

100 t ha^{-1} yr^{-1} (Table 5 and Figure 5b). The high (1000–1500 t ha^{-1}yr^{-1}) to very high (1500–2000 t ha^{-1}yr^{-1}) sediment yield categories together cover a larger area, collectively accounting for about 32.64% compared to the estimations (19%) made by the RUSLE, which are comparatively low. About 15.56% of the area is within the severe category,>200 t ha^{-1}yr^{-1}, concentrated in the northern part with a few pixels showing the severity in the central part. The distribution of the observed values can be explained in a manner similar to how it was described for the RUSLE output (Table 5 and Figure 5).

Both the models have emphasized the consistency in the distribution of soil loss and sediment yield, indicating that they encompass the same region when categorizing severity classes. In both the models, low severity class (<50 t ha^{-1}yr^{-1}) is found in low elevation zones and the class under severe erosion rate (>200 t ha^{-1}yr^{-1}) is concentrated at the upper reaches of the northern part, where the slope steepness and elevation are high. The high (100–150 t ha^{-1}yr^{-1}) to very high (150 to 200 t ha^{-1}yr^{-1}) class in both models is identified in regions characterized by a prevalence of streams, specifically along the edges of streams exhibiting high LS values.

In both the models, low severity class (<50 t ha^{-1}yr^{-1}) is found in low elevation zones and the class under severe erosion rate (>200 t ha^{-1}yr^{-1}) is concentrated at the upper reaches of the northern part, where the slope steepness and elevation are high. The high (100–150 t ha^{-1}yr^{-1}) to very high (150–200 t ha^{-1}yr^{-1}) class in both models is identified in regions characterized by a prevalence of streams, specifically along the edges of streams exhibiting high LS values. The few studies employing a single model (specifically RUSLE) have been published related to soil erosion in watersheds of Sikkim; however, the mentioned studies' multi-model approach has not been employed in the Sikkim region [60]. The consistency between both models indicates that the approach is correct and aligns with the outcomes of the study conducted by Ayele et al., where they used similar models [18]. The potential under very high to high risk of erosion depicts the spatial similarity in both models, whereas the average soil loss is comparatively low (RUSLE: 38 t/h/yr and SYI: 24 t/h/yr) in their study because of low elevation [18]. The findings using the Revised Universal Soil Loss Equation (RUSLE) and Sediment Yield Index (SYI) models, which estimate mean soil loss at 93.42 t ha^{-1} yr^{-1} and 70.3 t ha^{-1} yr^{-1}, respectively, and are consistent with previous research carried out in the same area and beyond. In contrast, Ahmed's study, which used the RUSLE and Sediment Delivery Ratio (SDR) models, calculated a mean annual soil loss of 126.89 t ha^{-1} yr^{-1} in the Dudhganga watershed ofKashmir Valley [84], which is within a comparable range but slightly higher than our results. Conversely, the research conducted by Dawa and Arjune, which implemented the RUSLE model over the whole state of Sikkim, documented a mean yearly soil erosion of 659 metric tons per hectare per year [85]. The discrepancy in the findings could be attributed to the fact that the aforementioned research encompassed the entire state of Sikkim, whereas our study specifically focuses on the South Sikkim district. The dominant factor contributing to the high soil loss rate is mainly attributed to the steepness of the slope and high elevation. In another study conducted by Naqvi et al., in a geographically analogous area to the current research, situated in the Uttarakhand Himalaya, the average annual soil loss was determined to be 1419.39 t ha^{-1}yr^{-1}, which is high, and their spatial pattern with respect to slope was very similar to the spatial pattern of soil loss results of this study [17]. It has been found that the high levels of soil erosion stem from the interplay of factors like steep terrain, Land Use and Land Cover alterations, and the exposure of bare soils resulting from human activities like agriculture and deforestation to make way for human settlements.

4. Conclusions

The comprehensive assessment of yearly soil erosion in South Sikkim, using the RUSLE and SYI models, has provided a valuable understanding of the root causes and factors that contribute to significant soil loss in the region. This research highlights the significant challenges posed by soil erosion in the area. The utilization of a multi-model technique for quantifying soil loss in this region is commendable, as no previous study has

employed two models to evaluate and compare the extent of severity in the Sikkim region. This investigation reveals that the soil erosion rate in South Sikkim is remarkably elevated. The average annual soil erosion rate for the region is around 93.42 metric tons per hectare per year for the RUSLE model and 70.3 metric tons per hectare per year for the SYI model. Both models have identified the same region in terms of severity categorization. This study also found a significant association between the severity of erosion rates in different zones (<50 to >200 tha^{-1} yr^{-1}) and certain topographical characteristics, such as steep slopes and high altitudes. These findings highlight the importance of considering topography and geomorphic features when assessing the risk of soil erosion. Hence, it is imperative to adopt soil conservation measures in these vulnerable regions such as non-tillage farming, cover cropping, and proper management of terraces to avert more soil degradation and safeguard the delicate ecosystem of this region. To reduce these issues, it is necessary to cover the surface with dense, deep-rooted tree vegetation [86]. Furthermore, this study provides a substantial foundation for policymakers and land managers to provide priority and develop effective erosion control measures in that geographical area. As a result, sustainable management of the region's natural resources and conservation of its valuable environment are promoted in order to maintain nature-based sustenance for the inhabitants of that location. But there is lack of temporal data as well as hydrometric stations for in-depth study of soil erosion and sediment loss. Therefore, this study would be appropriate as per the availability of data.

Author Contributions: Conceptualization, M.N. and H.R.N.; methodology, M.N.; software, M.N.; validation, H.R.N., M.N., and M.M.R.; formal analysis, M.M.R.; investigation; resources, P.K.M., K.A. and M.S.F.; data curation P.K.M., K.A., and M.S.F.; writing—original draft preparation, M.N. and H.R.N.; writing—review and editing, H.R.N., P.K.M., K.A., and M.S.F.; visualization, P.K.M., K.A., and M.S.F.; supervision, H.R.N., P.K.M., K.A., and M.S.F.; project administration, H.R.N., P.K.M., K.A., and M.S.F.; funding acquisition, P.K.M., K.A., and M.S.F. All authors have read and agreed to the published version of the manuscript.

Funding: Deep thanks and gratitude to the Researchers Supporting Project (RSP2024R249), King Saud University, Riyadh, Saudi Arabia, for funding this research article. This work was partially supported by ICSSR research grant (ICSSR-MOST (Taiwan)/IRP-4/2022-IC).

Data Availability Statement: The data are contained within the article.

Acknowledgments: We are thankful to all the agencies for providing datasets to carry out the research. Moreover, the roles of funding agencies (KSU, Riyadh & ICSSR-MOST) are highly acknowledged to support the research and publication.

Conflicts of Interest: The authors declare no conflicts of interest.

References

1. Pimentel, D. Soil erosion: A food and environmental threat. *Environ. Dev. Sustain.* **2006**, *8*, 119–137. [CrossRef]
2. Robinson, J.B.; Freebairn, D.M. Estimating changes in plant available soil water in broadacre cropping in Australia. *Water* **2017**, *1*, 1–4.
3. Owens, P.N.; Collins, A.J. (Eds.) *Soil Erosion and Sediment Redistribution in River Catchments: Measurement, Modelling and Management*; CABI: Wallingford, UK, 2006.
4. Naqvi, H.R.; Mohammed Abdul Athick, A.S.; Ganaie, H.A.; Siddiqui, M.A. Soil erosion planning using sediment yield index method in the Nun Nadi watershed, India. *Int. Soil Water Conserv. Res.* **2015**, *3*, 86–96. [CrossRef]
5. Lal, R. Soil erosion impact on agronomic productivity and environment quality. *Crit. Rev. Plant Sci.* **1998**, *17*, 319–464. [CrossRef]
6. Liu, B.; Zhang, X.; Wu, W.; Wang, X.; Zhang, Y. The assessment of soil loss by water erosion in China. *Int. Soil Water Conserv. Res.* **2020**, *8*, 430–439. [CrossRef]
7. Nearing, M.A.; Xie, Y.; Liu, B.; Ye, Y. Natural and anthropogenic rates of soil erosion. *Int. Soil Water Conserv. Res.* **2017**, *5*, 77–84. [CrossRef]
8. Montanarella, L. Agricultural Policy: Govern Our Soils. *Nature* **2015**, *528*, 32–33. [CrossRef]
9. Food and Agriculture Organization of the United Nations. European Soil Partnership Implementation Plan 2017–2020, 2017. Available online: http://www.fao.org/3/a-bs972e.pdf (accessed on 15 September 2024).
10. Stoddart, D.R. World Erosion and Sedimentation. In *Water, Earth, and Man*; Chorley, R., Ed.; Methuen: London, UK, 1969; pp. 43–64.

11. El-Swaify, S.A. State-of-the-art for assessing soil and water conservation needs and technologies. In *Adopting Conservation on the Farm: An International Perspective of the Socioeconomics of Soil and Water Conservation*; Soil and Water Conservation Society: Ankeny, IA, USA, 1994; pp. 13–27.
12. Dabral, P.P.; Baithuri, N.; Pandey, A. Soil erosion assessment in a hilly catchment of North Eastern India using USLE, GIS, and remote sensing. *Water Resour. Manag.* **2008**, *22*, 1783–1798. [CrossRef]
13. Senapati, U.; Das, T.K. Assessment of potential land degradation in Akarsa Watershed, West Bengal, using GIS and multi-influencing factor technique. In *Gully Erosion Studies from India and Surrounding Regions*; Springer: Cham, Switzerland, 2020; pp. 187–205. [CrossRef]
14. Patil, R.J.; Sharma, S.K.; Tignath, S.; Sharma, A.P.M. Use of remote sensing, GIS and C++ for soil erosion assessment in the Shakkar River basin, India. *Hydrol. Sci. J.* **2017**, *62*, 217–231. [CrossRef]
15. Raymo, M.E.; Ruddiman, W.F. Tectonic forcing of late Cenozoic climate. *Nature* **1992**, *359*, 117–122. [CrossRef]
16. Narayana, D.V.; Babu, R. Estimation of Soil Erosion in India. *J. Irrig. Drain. Eng.* **1983**, *109*, 419–434. [CrossRef]
17. Naqvi, H.R.; Mallick, J.; Devi, L.M.; Siddiqui, M.A. Multi-Temporal Annual Soil Loss Risk Mapping Employing Revised Universal Soil Loss Equation (RUSLE) Model in Nun Nadi Watershed, Uttrakhand (India). *Arab. J. Geosci.* **2013**, *6*, 4045–4056. [CrossRef]
18. Ayele, N.A.; Naqvi, H.R.; Alemayehu, D. Rainfall Induced Soil Erosion Assessment, Prioritization and Conservation Treatment Using RUSLE and SYI Models in Highland Watershed of Ethiopia. *Geocarto Int.* **2022**, *37*, 2524–2540. [CrossRef]
19. Nearing, M.A. Potential Changes in Rainfall Erosivity in the US with Climate Change during the 21st Century. *J. Soil Water Conserv.* **2001**, *56*, 229–232.
20. Wang, Y.; Wu, N.; Kunze, C.; Long, R.; Perlik, M. Drivers of change to mountain sustainability in the Hindu Kush Himalaya. In *The Hindu Kush Himalaya Assessment*; Wester, P., Mishra, A., Mukherji, A., Shrestha, A., Eds.; Springer: Cham, Switzerland, 2019; pp. 17–56. [CrossRef]
21. Adhikari, K.; Hartemink, A.E. Linking soils to ecosystem services—A global review. *Geoderma* **2016**, *262*, 101–111. [CrossRef]
22. Qiu, L.; Zhang, Q.; Zhu, H.; Reich, P.B.; Banerjee, S.; van der Heijden, M.G.; Sadowsky, M.J.; Ishii, S.; Jia, X.; Shao, M.; et al. Erosion reduces soil microbial diversity, network complexity and multifunctionality. *ISME J.* **2021**, *15*, 2474–2489. [CrossRef]
23. Borrelli, P.; Robinson, D.A.; Fleischer, L.R.; Lugato, E.; Ballabio, C.; Alewell, C.; Meusburger, K.; Modugno, S.; Schütt, B.; Ferro, V.; et al. An assessment of the global impact of 21st century land use change on soil erosion. *Nat. Commun.* **2017**, *8*, 2013. [CrossRef] [PubMed]
24. Kathuria, V.; Balasubramanian, R. The environmental cost of using top-soil for brick-making: A case study from Tamil Nadu, India. *Rev. Mark. Integr.* **2013**, *5*, 171–201. [CrossRef]
25. Jain, S.K.; Roshan, A.D.; Arlekar, J.N.; Basu, P.C. Empirical attenuation relationships for the Himalayan earthquakes based on Indian strong motion data. In Proceedings of the Sixth International Conference on Seismic Zonation, Palm Springs, CA, USA, 12–15 November 2000; pp. 12–15.
26. ICIMOD. *Constraints and Opportunities. Proceedings of the International Symposium on Mountain Environment and Development*; International Centre for Integrated Mountain Development (ICIMOD): Kathmandu, Nepal, 1994.
27. Naqvi, H.R.; Devi, L.M.; Siddiqui, M.A. Soil loss prediction and prioritization based on revised universal soil loss estimation (RUSLE) model using geospatial technique. *Int. J. Environ. Prot.* **2012**, *2*, 39–43.
28. Poręba, G.J.; Prokop, P. Estimation of soil erosion on cultivated fields on the hilly Meghalaya Plateau, North-East India. *Geochronometria* **2011**, *38*, 77–84. [CrossRef]
29. Sharda, V.N.; Ojasvi, P.R. A revised soil erosion budget for India: Role of reservoir sedimentation and land-use protection measures. *Earth Surf. Process. Landf.* **2016**, *41*, 2007–2023. [CrossRef]
30. Naqvi, H.R.; Athick, A.M.A.; Siddiqui, L.; Siddiqui, M.A. Multiple modeling to estimate sediment loss and transport capacity employing hourly rainfall and In-Situ data: A prioritization of highland watershed in Awash River basin, Ethiopia. *Catena* **2019**, *182*, 104173. [CrossRef]
31. García-Ruiz, J.M.; Beguería, S.; Nadal-Romero, E.; González-Hidalgo, J.C.; Lana-Renault, N.; Sanjuán, Y. A meta-analysis of soil erosion rates across the world. *Geomorphology* **2015**, *239*, 160–173. [CrossRef]
32. Jetten, V.; Govers, G.; Hessel, R. Erosion Models: Quality of Spatial Predictions. *Hydrol. Earth Syst. Sci.* **2003**, *17*, 887–900. [CrossRef]
33. Karydas, C.G.; Panagos, P.; Gitas, I.Z. A classification of water erosion models according to their geospatial characteristics. *Int. J. Digit. Earth* **2014**, *7*, 229–250. [CrossRef]
34. Wischmeier, W.H.; Smith, D.D. *Prediction Rainfall Erosion Losses: A Guide to Conservation, Agricultural Handbook 537*; Planning, Science and Education Administration, US Department of Agriculture: Washington, DC, USA, 1978; 58p.
35. Renard, K.G.; Foster, G.R.; Weesies, G.A.; McCool, D.K.; Yoder, D.C. *Predicting Soil Erosion by Water: A Guide to Conservation Planning with the Revised Universal Soil Loss Equation (RUSLE)*; Agriculture Handbook No. 703; USDA-ARS: Washington, DC, USA, 1997.
36. Williams, J.R. *Sediment Yield Prediction with Universal Equation Using Runoff Energy Factor*; ARS-S-40; USDA: Washington, DC, USA, 1975; pp. 244–252.
37. Flanagan, D.C.; Nearing, M.A. USDA-Water Erosion Prediction Project: Hillslope profile and watershed model documentation. *Nserl Rep.* **1995**, *10*, 1–123.

38. All India Soil and Land Use Survey (AISLUS). Priority Delineation, Matatilla RVP, U.P. Report No. Agri.484. 1977. Available online: https://slusi.da.gov.in/aboutslusi.html (accessed on 15 September 2024).
39. Arnold, J.G.; Srinivasan, R.; Muttiah, R.S.; Williams, J.R. Large Area Hydrologic Modeling and Assessment. Part I: Model Development. *J. Am. Water Resour. Assoc.* **1998**, *34*, 73–89. [CrossRef]
40. Panagos, P.; Borrelli, P.; Poesen, J.; Ballabio, C.; Lugato, E.; Meusburger, K.; Montanarella, L.; Alewell, C. The new assessment of soil loss by water erosion in Europe. *Environ. Sci. Policy* **2015**, *54*, 438–447. [CrossRef]
41. Rajbanshi, J.; Bhattacharya, S. Assessment of soil erosion, sediment yield and basin specific controlling factors using RUSLE-SDR and PLSR approach in Konar river basin, India. *J. Hydrol.* **2020**, *587*, 124935. [CrossRef]
42. Perera, D.; Williams, S.; Smakhtin, V. Present and future losses of storage in large reservoirs due to sedimentation: A country-wise global assessment. *Sustainability* **2023**, *15*, 219. [CrossRef]
43. Osipov, A.F.; Bobkova, K.S.; Dymov, A.A. Carbon stocks of soils under forest in the Komi Republic of Russia. *Geoderma Reg.* **2021**, *27*, e00427. [CrossRef]
44. Shrestha, D.P. Assessment of soil erosion in the Nepalese Himalaya: A case study in LikhuKhola Valley, Middle Mountain Region. *Land Husb.* **1997**, *2*, 59–80.
45. Maetens, W.; Vanmaercke, M.; Poesen, J.; Jankauskas, B.; Jankauskiene, G.; Ionita, I. Effects of land use on annual runoff and soil loss in Europe and the Mediterranean: A meta-analysis of plot data. *Prog. Phys. Geogr.* **2012**, *36*, 599–653. [CrossRef]
46. Prasannakumar, V.; Vijith, H.; Abinod, S.; Geetha, N.J.G.F. Estimation of soil erosion risk within a small mountainous sub-watershed in Kerala, India, using Revised Universal Soil Loss Equation (RUSLE) and geo-information technology. *Geosci. Front.* **2012**, *3*, 209–215. [CrossRef]
47. Pan, J.; Wen, Y. Estimation of soil erosion using RUSLE in Caijiamiao watershed, China. *Nat. Hazards* **2014**, *71*, 2187–2205. [CrossRef]
48. Mandal, D.; Sharda, V.N. Appraisal of soil erosion risk in the Eastern Himalayan region of India for soil conservation planning. *Land Degrad. Dev.* **2013**, *24*, 430–437. [CrossRef]
49. Uddin, K.; Murthy, M.S.R.; Wahid, S.M.; Matin, M.A. Estimation of soil erosion dynamics in the Koshi basin using GIS and remote sensing to assess priority areas for conservation. *PLoS ONE* **2016**, *11*, e0150494. [CrossRef]
50. Lal, R.; Blum, W.H.; Valentine, C.; Stewart, B.A. *Methods for Assessment of Soil Degradation*; CRC Press: Boca Raton, FL, USA, 1997.
51. Galdino, S.; Sano, E.E.; Andrade, R.G.; Grego, C.R.; Nogueira, S.F.; Bragantini, C.; Flosi, A.H. Large-scale modeling of soil erosion with RUSLE for conservationist planning of degraded cultivated Brazilian pastures. *Land Degrad. Dev.* **2016**, *27*, 773–784. [CrossRef]
52. Kumar, R.; Naqvi, H.R.; Devrani, R.; Deshmukh, B.; Huang, J.C. Sediment yield assessment, prioritization and control practices in Chambal River basin employing SYI model. *J. Geol. Soc. India* **2022**, *98*, 1585–1594. [CrossRef]
53. Delmas, M.; Calvet, M.; Gunnell, Y. Variability of Quaternary glacial erosion rates–A global perspective with special reference to the Eastern Pyrenees. *Quat. Sci. Rev.* **2009**, *28*, 484–498. [CrossRef]
54. Gajbhiye, S. Estimation of surface runoff using remote sensing and geographical information system. *Int. J. U-E Serv. Sci. Technol.* **2015**, *8*, 113–122. [CrossRef]
55. AISLUS. *Methodology for Priority Delineation Survey*; All India Soil and Land Use Survey, Ministry of Agriculture, Government of India: New Delhi, India, 1991.
56. Sati, S.P.; Sundriyal, Y.P.; Rana, N.; Dangwal, S. Recent landslides in Uttarakhand: Nature's fury or human folly. *Curr. Sci.* **2011**, *100*, 1617–1620.
57. Boardman, J. Soil erosion science: Reflections on the limitations of current approaches. *Catena* **2006**, *68*, 73–86. [CrossRef]
58. Borrelli, P.; Alewell, C.; Alvarez, P.; Anache, J.A.A.; Baartman, J.; Ballabio, C.; Panagos, P. Soil erosion modelling: A global review and statistical analysis. *Sci. Total Environ.* **2021**, *780*, 146494. [CrossRef]
59. Farhan, Y.; Zregat, D.; Farhan, I. Spatial estimation of soil erosion risk using RUSLE approach, RS, and GIS techniques: A case study of Kufranja watershed, Northern Jordan. *J. Water Resour. Prot.* **2013**, *5*, 1247–1261. [CrossRef]
60. Chatterjee, N. Soil erosion assessment in a humid, Eastern Himalayan watershed undergoing rapid land use changes, using RUSLE, GIS and high-resolution satellite imagery. *Model. Earth Syst. Environ.* **2020**, *6*, 533–543. [CrossRef]
61. Hanel, M.; Maca, P.; Basta, P.; Vlnas, R.; Pech, P. Rainfall erosivity factor in the Czech Republic and its uncertainty. *Hydrol. Earth Syst. Sci.* **2016**, *20*, 4307–4322. [CrossRef]
62. Foster, G.R.; Yoder, D.C.; Weesies, G.A.; McCool, D.K.; McGregor, K.C.; Bingner, R.L. *Draft User's Guide, Revised Universal Soil Loss Equation Version 2 (RUSLE-2)*; USDA-Agricultural Research Service: Washington, DC, USA, 2003.
63. Verstraeten, G.; Poesen, J.; Demaree, G.; Salles, C. Long–term (105 years) variability in rain erosivity as derived from 10–min rainfall depth data for Ukkel (Brussels, Belgium), Implications for assessing soil erosion rates. *J. Geophys. Res.* **2006**, *111*, 22. [CrossRef]
64. Arnoldus, H.M.J. An approximation of the rainfall factor in the universal soil loss equation. In *Assessment of Erosion*; De Boodt, M., Gabriels, D., Eds.; John Wiley & Sons: Chichester, UK, 1980; pp. 127–132.
65. Erencin, Z.; Shresta, D.P.; Krol, I.B. C-Factor Mapping Using Remote Sensing and GIS. Case Study LomSakLom Kao ThailGeogrInst Justus-Liebig-UnivGiess Intern InstAerospSurv Earth SciITCEnschede Netherland, 2000. Available online: https://d-nb.info/1050225775/34 (accessed on 15 September 2024).

66. Sharpley, A.N.; Williams, J.R. *EPIC-Erosion/Productivity Impact Calculator. I: Model Documentation. II: User Manual*. Technical Bulletin-United States Department of Agriculture. 1990. Available online: https://agrilife.org/epicapex/files/2015/05/EpicModelDocumentation.pdf (accessed on 15 September 2024).
67. Sharon, D. The distribution of hydrologically effective rainfall incident on sloping ground. *J. Hydrol.* **1980**, *46*, 165–188. [CrossRef]
68. Lastoria, B.; Miserocchi, F.; Lanciani, A.; Monacelli, G. An estimated erosion map for the Aterno-Pescara river basin. *Eur. Water* **2008**, *21*, 29–39.
69. Moore, I.D.; Burch, G.J. The physical basis of the length-slope factor in the universal soil loss equation. *Soil Sci. Soc. Am. J.* **1986**, *50*, 1294–1298. [CrossRef]
70. Moore, I.D.; Burch, G.J. Modeling erosion and deposition: Topographic effects. *Trans. Am. Soc. Agric. Eng.* **1986**, *26*, 1624–1630. [CrossRef]
71. Karydas, C.G.; Sekuloska, T.; Silleos, G.N. Quantification and site-specification of the support practice factor when mapping soil erosion risk associated with olive plantations in the Mediterranean island of Crete. *Environ. Monit. Assess.* **2009**, *149*, 19–28. [CrossRef]
72. Colman, C.B. *Impacts of climate and land use changes on soil erosion in the Upper Paraguay Basin*; Federal University of Mato Grosso do Sul: Campo Grande, Brazil, 2018.
73. Bruijnzeel, L.A. Hydrological functions of tropical forests: Not seeing the soil for the trees? *Agric. Ecosyst. Environ.* **2004**, *104*, 185–228. [CrossRef]
74. Shaikh, M.S.; Shetkar, R.V. Soil Erosion Estimation Modelling by Revised Universal Soil Loss Equation and Soil and Water Assessment Tool on Geographic Information System Platform. *J. Water Resour. Eng. Manag.* **2018**, *5*, 2.
75. Williams, J.R.; Berndt, H.D. Sediment yield computed with universal equation. *Proc. ASCE* **1972**, *98*, 2087–2098. [CrossRef]
76. Kouli, M.; Soupios, P.; Vallianatos, F. Soil erosion prediction using the revised universal soil loss equation (RUSLE) in a GIS framework, Chania, Northwestern Crete, Greece. *Environ. Geol.* **2009**, *57*, 483–497. [CrossRef]
77. Liu, B.Y.; Nearing, M.A.; Shi, P.J.; Jia, Z.W. Slope Length Effects on Soil Loss for Steep Slopes. *Soil Sci. Soc. Am. J.* **2000**, *64*, 1759–1763. [CrossRef]
78. Fan, J.C.; Wu, M.F. Estimation of interrill soil erosion on steep slopes. *Trans. ASABE* **2001**, *44*, 1471.
79. Ganasri, B.P.; Ramesh, H. Assessment of soil erosion by RUSLE model using remote sensing and GIS-A case study of Nethravathi Basin. *Geosciences* **2016**, *7*, 953–961. [CrossRef]
80. Colman, C.B.; Garcia, K.M.P.; Pereira, R.B.; Shinma, E.A.; Lima, F.E.; Gomes, A.O.; Oliveira, P.T.S. Different approaches to estimate the sediment yield in a tropical watershed. *RBRH* **2018**, 23. [CrossRef]
81. Rawat, K.S.; Tripathi, V.K.; Mishra, A.K. Sediment yield index mapping and prioritization of Madiasubwatershed, Sagar District of Madhya Pradesh (India). *Arab. J. Geosci.* **2014**, *7*, 3131–3145. [CrossRef]
82. Gajbhiye, S.; Sharma, S.K.; Meshram, C. Prioritization of watershed through sediment yield index using RS and GIS approach. *Int. J. U-E-Serv. Sci. Technol.* **2014**, *7*, 47–60. [CrossRef]
83. Lohar, T.; Balasubramani, K.; Bhatt, B. Site Suitability for Establishing Soil and Water Conservation Structures Using Geoinformatics–A Case Study of Chinnar Watershed, Tamil Nadu, India. *J. Geomat.* **2018**, *12*, 146–257.
84. Ahmad, W.S.; Jamal, S.; Taqi, M.; El-Hamid, H.T.A.; Norboo, J. Estimation of soil erosion and sediment yield concentrations in Dudhganga watershed of Kashmir Valley using RUSLE & SDR model. *Environ. Dev. Sustain.* **2024**, *26*, 215–238.
85. Dawa, D.; Arjune, V. Identifying Potential Erosion-Prone Areas in the Indian Himalayan Region Using the Revised Universal Soil Loss Equation (RUSLE). *Asian J. Water Environ. Pollut.* **2021**, *18*, 15–23. [CrossRef]
86. Singh, J.S.; Pandey, A.N.; Pathak, P.C. A hypothesis to account for the major pathways of soil loss from Himalaya. *Environ. Conserv.* **1983**, *10*, 343–345. [CrossRef]

Disclaimer/Publisher's Note: The statements, opinions and data contained in all publications are solely those of the individual author(s) and contributor(s) and not of MDPI and/or the editor(s). MDPI and/or the editor(s) disclaim responsibility for any injury to people or property resulting from any ideas, methods, instructions or products referred to in the content.